Plasma Medicine, 1(1): 45–54 (2011)

Targeted Cancer Treatment Using Anti-EGFR and -TFR Antibody-Conjugated Gold Nanoparticles Stimulated by Nonthermal Air Plasma

G. J. Kim,[1] S. R. Park,[2] G. C. Kim,[2]* & J. K. Lee[1]

[1]Department of Electronic and Electrical Engineering, Pohang University of Science and Technology. [2]Department of Oral Anatomy, School of Dentistry, Pusan National University

*Address all correspondence to: G. C. Kim, Department of Oral Anatomy, School of Dentistry, Pusan National University, Busan 602-739, Republic of Korea; ki91000m@pusan.ac.kr

ABSTRACT: Nonthermal air plasma killed G361 melanoma and SCC25 oral cancer cells targeted by antibody-conjugated gold nanoparticles. Although plasma alone is effective in killing cancerous cells, it also affects normal cells during the treatment process. For enhanced effects, gold nanoparticles and cancer-specific antibodies were pretreated before plasma treatment. Gold nanoparticles taken up by the cancerous cells are stimulated by the plasma treatment. Stimulation of gold nanoparticles results in an increase in death rate of cancerous cells. The selectivity of the killing process is achieved by conjugating gold nanoparticles with antiepidermal growth factor receptor and transferrin receptor antibodies. These conjugates can bind specifically to cancer cells. Gold nanoparticles stimulated by plasma kill these cancerous cells effectively. In this way, the killing efficiency of the plasma treatment process in the presence of conjugates is amplified about 18 times compared to the plasma treatment in the absence of conjugates. This technique shows the possibility of using plasma therapy for killing cancer cells selectively and effectively.

I. INTRODUCTION

Human oral squamous carcinoma (OSC) and melanoma are oral cavity cancers. Especially, OSC is responsible for the majority of malignancies in the oral cavity. The conventional methods for the treatment of oral cavity cancers are based on surgical extirpation, radiation, chemotherapy, or a combination of these treatments. These methods have some limitations. For example, surgical removal of oral cancer can result in facial distortion with physical and psychological consequences. Use of chemotherapy is limited due to its side effects (toxicity) and the development of high resistance to chemotherapeutic agents at later stages of malignancy.[1] Therefore, the treatment of OSC oral cancer cells favors the use of new methodologies that are not only effective in killing cancerous cells, but also must be selective so that normal cells remain undisturbed during the treatment.

Recently, it has been shown that well-designed nonthermal plasmas are effective in killing cancer cells.[2] Plasma alone, however, is unable to achieve selectivity because it kills both normal and cancerous cells. Recent advances in nanotechnology have resulted in the use of gold nanoparticles as diagnostic and drug delivery tools.[3,4] More applica-

2151-805X/11/$35.00 © 2011 by Begell House, Inc.

tions of gold nanoparticles are found in cancer therapy when the plasma interacts with gold nanoparticles. Gold nanoparticles can be used by conjugating with a cancer-specific antibody to achieve the selectivity in plasma treatment. Conjugated nanoparticles can bind selectively to target cells, which are then affected by the plasma. In this regard, we have previously demonstrated the enhanced effects of antifocal adhesion kinase (FAK) conjugates and plasma.[5]

In this study, we have further investigated the synergistic effect of gold conjugates and plasma for the selective treatment of oral squamous carcinoma cells. In many oral cancer cells, the epidermal growth receptor (EGFR) and transferrin receptor (TFR) have been known to be overexpressed. These receptors are regarded as an attractive target for cancer therapy.[6–8] Therefore, anti-EGFR antibody and anti-TFR antibodies were conjugated to gold nanoparticles for targeting oral cancer.

II. MATERIALS AND METHODS

A. Nonthermal Air Plasma Source

Figure 1A shows the schematic diagram of the experimental setup. The plasma source was designed to operate in ambient air with 22 kHz, with a few kilovolt sinusoidal voltage source. The plasma source consists of a polytetrafluoroethylene (PTFE) dielectric and Cu electrodes on both sides of the PTFE. The plasma source was a Cu-PTFE-Cu stacked structure of circuit board. The electrode structure was formed by a conventional chemical etching process. The plasma was generated by the fringing field near the front-face electrode.[9] Figure 1B shows voltage and current waveforms of the plasma device. A high-voltage probe (Tektronix P6015A) and a current probe (Pearson current monitor Model 4100) were used. The capacitive load of the plasma source made the voltage lead the current waveform 90 deg in phase. An applied voltage of 4.2 kV (rms) induced the typical DBD type current waveform, showing several current peaks in positive rising and negative falling times of the voltage waveform due to the accumulation of charges on the dielectric surface. These random current peaks result from movement of charged particles in a very short time (~nanoseconds), which is a characteristic of filamentary discharges. Making plasma consumed 4.26 W, as calculated from the measured voltage and current waveforms. For the 40 s treatment, an energy density of about 27 J/cm^2 was estimated within the area of the plasma.

Optical emission spectroscopy was used to find the rotational temperature of the discharge. An optical emission spectrometer, consisting of a 750 mm focal length monochromator (Dong Woo Optron Co. Ltd. 750, Monora 750i) with a built-in high-sensitivity photomultiplier tube (PMT, R928 Hamamatsu) and a grating 2400 gr/mm blazed at 240 nm was utilized. The second positive system of nitrogen dominated in the 300–400 nm range. The rotational temperature of the second positive nitrogen C-B transition bands was also analyzed (Fig. 2B). To find the optimum fit between measured and simulated spectrums, the technique described by Phillips[10] was used. The inset of Figure 2B shows how the optimum fit was found by varying the estimated rotational

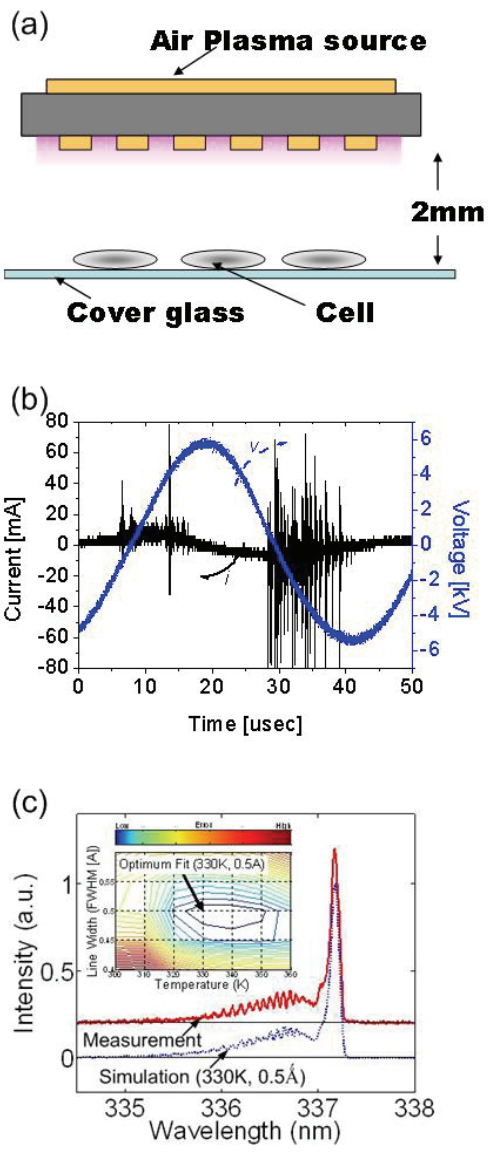

FIGURE 1. Plasma source. (A) Schematic diagram of experiment. (B) Current and voltage waveforms of plasma source. (C) Rotational temperature of plasma source.

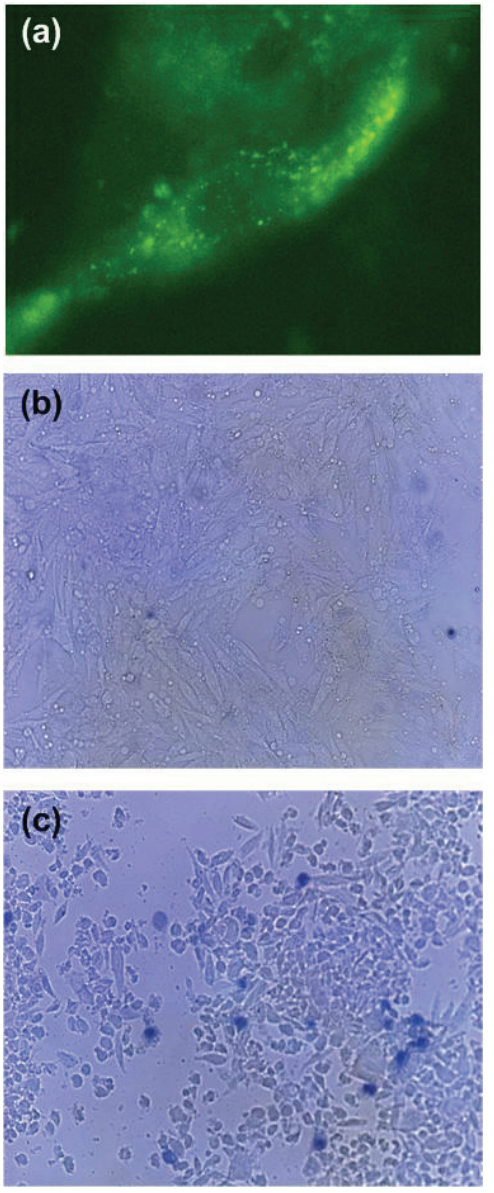

FIGURE 2. Plasma treatment on the G361 cells. (A) Uptake of gold nanoparticles. (B) Plasma treatment without gold nanoparticles. (C) Plasma treatment with gold nanoparticles

temperature and line width. Finally, the rotational temperature of the discharge was determined to be 330 K, and this value agrees with the temperature determined near the plasma source by the fiber optic temperature measurement technique.

B. Cell Culture

Human melanoma (G361), human tongue squamous carcinoma (SCC25), and mouse fibroblast (NIH3T3) cell lines were purchased from the ATCC (Rockville, Maryland). These cells were grown in Dulbecco's modified eagle's medium supplemented with 25 mM HEPES, 100 μg/ml penicillin/streptomycin, 4 mM L-glutamine, and 10% fetal bovine serum at 37°C in a 5% CO2 humidified-air incubator.

C. Plasma Treatment and Cell Viability Assay

After 4×10^5 G361 and SCC25 cells were incubated on cover slips for 24 hr, cover slips without media were placed 2 mm from the plasma source and exposed to a 30 s plasma treatment. Cells treated with plasma were washed immediately with phosphate buffered saline (PBS), stained with trypan blue, and then counted using a hemocytometer.

D. Immunocytochemistry

Cells were treated with the mouse anti-TFR (anti-EGFR) antibody-conjugated gold nanoparticles (TFR-GNPs, EGFR-GNPs) and then fixed in 4% paraformaldehyde for 10 min. Cells were permeabilized with 0.2% Triton X-100 in PBS for 10 min and then incubated with goat FITC-antimouse secondary antibody for 1 hr. Samples were observed under a fluorescence microscope (Axioskop, Zeiss, Germany).

E. Conjugation

An aqueous solution of 11-mercaptoundecanoic acid (MUA) (0.1 mg/ml) was added to the colloidal gold suspension and incubated overnight. MUA-modified gold nanoparticles were reacted with a mixture of 1 mM N-hydroxysuccinimide (NHS) and 1 mM N-ethyl-N'-(3-dimethylaminopropyl) carbodiimide (EDC) solution for 20 min. NHS-terminated gold nanoparticles were incubated with 250 μg/ml anti- EGFR anti-TFR antibodies in PBS buffer (1 mM, pH 7.0) for 6 hr.

F. Western Blot

Cells were lysed in ice-cold lysis buffer [300 mM NaCl, 50 mM Tris-Cl (pH 7.6), 0.5% TritonX-100, 2 mM PMSF, 2 μl /ml aprotinin, and 2 μl /ml leupeptin] and incubated at 4°C for 30 min. A quantity of 5c μg of proteins were loaded onto 7.5% SDS/PAGE. The gels were transferred to a nitrocellulose membrane and reacted with anti-EGFR and anti-TFR antibodies (Santa Cruz Biotechnology, Inc.). Immunostaining was performed using SuperSignal West Pico enhanced chemiluminescence substrate and detected with LAS-3000PLUS (Fuji Photo Film Company, Kanagawa, Japan).

III. RESULTS AND DISCUSSION

In order to see the synergistic effect of gold conjugates and plasma, it was required to verify the uptake of gold nanoparticles by cancer cells. Figure 2A shows an immunostaining image of the G361 human melanoma skin cancer cells after 24 hr incubation with 30 nm gold nanoparticles. Green fluorescence was taken under the fluorescent microscope due to a fluorescein conjugated, affinity-purified secondary antibody, which was made to bind with the gold nanoparticles. The figure shows spindle shape cell morphology and a nucleus surrounded by cytosol where a lot of gold nanoparticles reside. The colloidal gold nanoparticles can get into and out of the cell during the metabolism. A part of gold nanoparticles, which remained for 24 hr incubation, was observed. In this case, the gold nanoparticles can be placed within the cytosol. The position of gold nanoparticles can be controlled by binding the gold nanoparticles with the specific antibodies.

To show that plasma can stimulate the gold nanoparticles inside of the cell, G361 melanoma cancer cells were treated with the plasma for 30 s following 24 hr incubation together with colloidal gold nanoparticles. Figure 2 shows trypan blue–stained cells after the plasma treatment without (Fig. 2B) and with (Fig. 2C) gold nanoparticles. In the case of treatment with gold nanoparticles (Fig. 2C), the cell morphology was changed to a round shape and cells formed aggregates. On the other hand, when treatment was performed without gold nanoparticles, the cells retained their shape.

In order to obtain quantitative results after the plasma treatment, all treated cells were harvested, stained with trypan blue, and counted with a hemocytometer. Figure 3A shows the death rate and proliferation (growth) rate of G361 melanoma cells after plasma treatment with and without colloidal gold nanoparticles. In the case of low-dose plasma exposure (4.5 kV), the cell death rate for the two kinds of treatment (with and without gold nanoparticles) was not significantly different. However, when the applied voltage was increased, the death rate increased significantly in the cells treated with gold nanoparticles. When gold nanoparticles were used, the death rate increased more than twice (from 14% to 36%) immediately after the plasma stimulation. This shows that plasma stimulates gold nanoparticles to attack cancer cells. This also implies that addition of gold nanoparticles can reduce the required voltage for effective cell killing and improves the selectivity of plasma treatment. It must be noted that gold nanoparticles became effective after being exposed to plasma. If the cells in the presence of gold nanoparticles are not treated with plasma, gold nanoparticles have no effect on the cells.

We assumed that low-dosed plasma treatment would have no effect on the immediate death rate after plasma treatment. However, when the number of cells was checked 24 hr after the plasma treatment, the cell proliferation was significantly reduced. Figure 3B summarizes the proliferation rates of G361 cells with and without gold nanoparticles with 24 hr incubation after the plasma exposure. The plasma treatment of cells without gold nanoparticles decreased the proliferation rate to 54%. However, the proliferation rate of cells with gold nanoparticles was reduced to 15% after plasma treatment. This

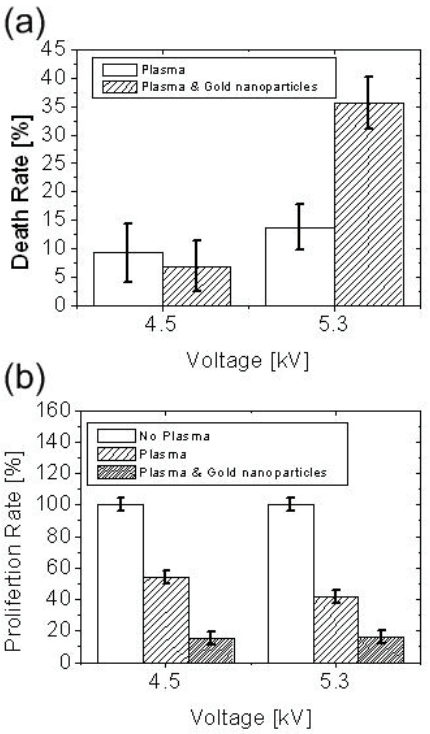

FIGURE 3. Effects of plasma exposure on G361 cells. (A) Cell death rate. (B) Proliferation rate.

indicates the therapeutic value of plasma alone and synergetic effect of plasma and gold nanoparticles for cancerous cell treatment.

To further investigate, gold nanoparticles were conjugated with EGFR and TFR. The EGFR is a transmembrane glycoprotein that constitutes one of four members of the erbB family of tyrosine kinase receptors (170 kDa). Binding of EGFR to its conjugate ligands leads to autophosphorylation of receptor tyrosine kinase and subsequent activation of signal transduction pathways that are involved in regulating cellular proliferation, differentiation, and survival. Although EGFR is present in normal cells, it is overexpressed in a variety of tumor cell lines, and has been associated with poor prognosis and decreased survival. EGFR activation also plays a role in resistance to chemotherapy and radiation treatment in tumor cells. Over the past two decades, much of chemotherapy research has focused on developing anticancer agents that can obstruct EGFR activity.[11–13] The TFR is a cell membrane–associated glycoprotein involved in the cellular uptake of iron and in the regulation of cell growth. Iron uptake occurs via the internalization of iron-loaded transferrin mediated by the interaction with the TFR.[1] It is reported that the expression level of TFR in cancer cells may be up to 100-fold higher than average expression level

of TFR in normal cells. The high expression level of TFR in cancer cells and its central role in the cellular pathology of human cancer make this receptor an attractive target for cancer therapy.[2] Therefore, targeting the TFR is a promising strategy actively being explored as a drug alternative to offset dangerous side effects. Figure 4 shows the high expression of EGFR and TFR in SCC25 oral squamous carcinoma cells compared with NIH 3T3 normal cells. This suggests that both receptors could be suitable for target proteins.

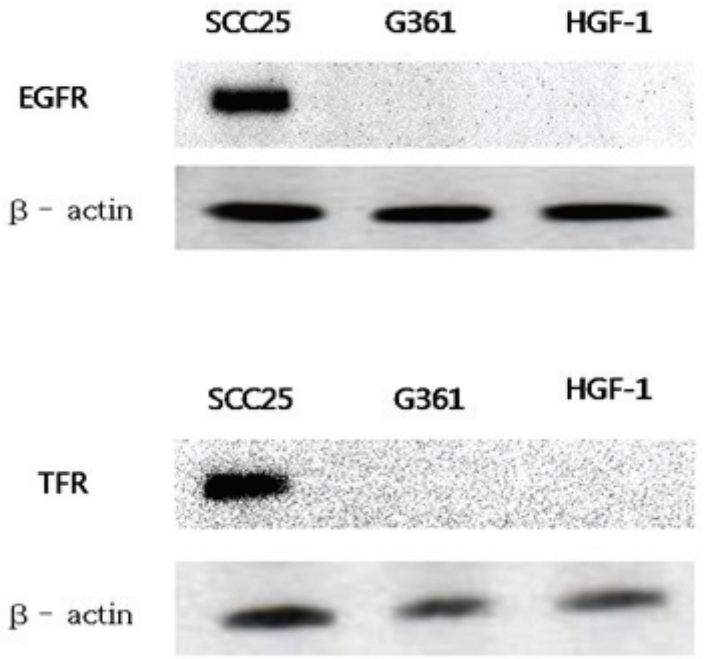

FIGURE 4. Western blotting analysis for EGFR and TFR in different cells. (A) Expression level of EGFR. (B) Expression level of TFR. β-actin was used for loading control.

The uptake of conjugates was observed before plasma treatment. Figure 5 shows the binding images of EGFR-GNP and TFR-GNP conjugates on the SCC25 cells. Figures 5A and 5B show EGFR-GNP conjugates, while Figures 5C and 5D show TFR-GNP conjugates. The green fluorescence of Figures 5A and 5C detected gold conjugates, while Figures 5B and 5D show corresponding phase contrast images. Because the EGFR and TFR are located on the cell membrane, the uptake images look like a shell covering cell membrane. It is important to mention that the attachment of gold nanoparitcles on the cells can be controlled by selecting an appropriate antibody for conjugates. The colloidal

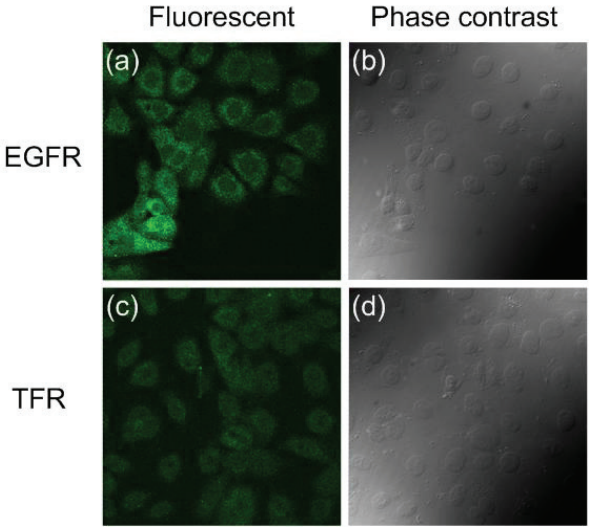

FIGURE 5. Immunocytochemistry. (A) Fluorescent image of SCC25 cells binding with EGFR conjugates. (B) Phase contrast image of (A). (C) Fluorescent image of SCC25 cells binding with TFR conjugates. (D) Phase contrast image of (C).

gold nanoparticles reside within the cytosol (Fig. 2A), while EGFR-GNP and TFR-GNP conjugates surround the cell membrane (Fig. 5).

In order to confirm the lethal effect of plasma plus EGFR-GNP or TFR-GNP, cells were divided into four groups: cells cultured in pure media (Fig. 6A); cells cultured in media containing gold nanoparticles (Fig. 6B); cells cultured in media containing TFR-GNP (Fig. 6C); and cells cultured in media containing EGFR-GNP (Fig. 6D). When these four groups of cells were treated by plasma for 30 s, the death rates were 5%, 21%, 66%, and 92%, respectively (Fig. 6E). In the case of cells treated with TFR-GNP, although the death rate right after plasma treatment was 66%, most alive cells were finally dead after 4 h incubation. Considering the instant death rate of 92% in the EGFR-GNP–treated group, the death mechanism might be necrosis, whereas in the TFR-GNP–treated group, apoptosis might be induced for 4 hr as well as necrosis. In our preliminary research, human normal gingival fibroblast showed a 5% death rate (data not shown) when they were treated with TFR-GNP and EGFR-GNP plus plasma, because they did not express TFR and EGFR on the cell surface (Fig. 4). While the death rate of the control group was 5%, those of TFR-GNP and EGFR-GNP were about 13-fold and 18-fold higher, suggesting that the combination treatment of plasma and TFR-GNP or EGFR-GNP has a strong selective treatment of SCC25 cells. Although the present results are promising, it is unclear how plasma stimulates GNP or what exact death mechanism was involved. Thus, those mechanisms are expected to be traced in the next research.

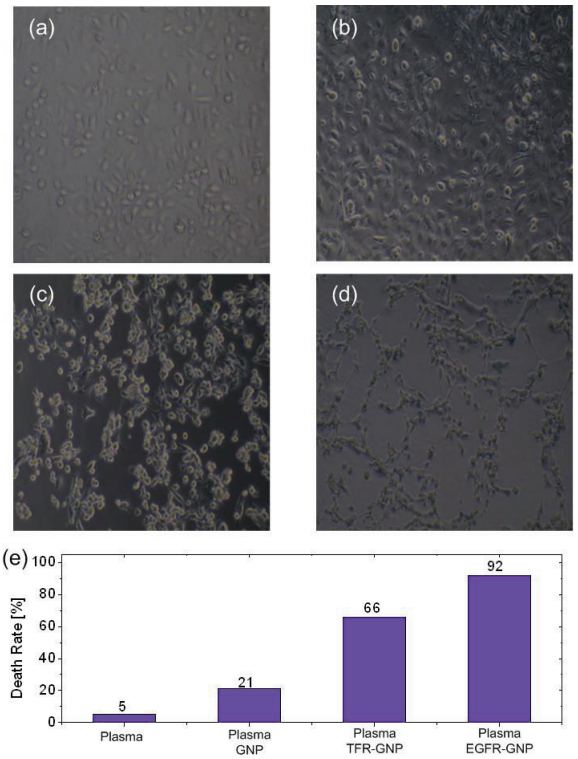

FIGURE 6. Enhancement of cell death by plasma treatment plus TFR-GNP and EGFR-GNP in SCC25 cells. (A) Control cells. (B) Cells treated with colloidal gold nanoparticles. (C) Cells treated with TFR-GNP. (D) Cells treated with EGFR-GNP. (E) Death rates.

IV. SUMMARY

In this work, we have proposed a nonthermal air plasma coupled with antibody conjugated gold nanoparticles for selective and effective melanoma and oral cancer therapy. In the absence of conjugated gold nanoparticles, nonthermal air plasma kills cancerous cells effectively, and its use results in reduction of proliferation rate, however, it also affects normal cells. This problem of killing normal cells by nonthermal air plasma can be taken care of by using gold nanoparticles. It shows that cells incubated with gold nanoparticles are vulnerable to plasma treatment. It is also shown that the efficiency of the treatment process can be enhanced when the gold nanoparticles are conjugated with anti-EGFR and anti-TFR antibodies. In the presence of EGFR-GNP conjugates, the treatment process became about 18 times more efficient as compared to the case when the plasma alone is used for treatment of cancerous cells. These results suggest that the attack against TFR and/or EGFR by means of plasma may be a prominent strategy for oral carcinoma cells.

ACKNOWLEDGMENTS

This work was supported by the Korea Science and Engineering Foundation (KOSEF) Grant No. R01-2007-000-10730-0 and the Brain Korea 21 program funded by the Korean Ministry of Education, Science, and Technology. This work was supported by the Institute for Research & Industry Cooperation of the Pusan National University (PNUIRIC, Research Development Promotion Fund) (Grant No. PNUIRIC-2009-201-○○○○○○)

REFERENCES

1. D'Silva NJ, Ward BB. Tissue biomarkers for diagnosis & management of oral squamous cell carcinoma. Alpha Omegan. 2007;100(4):182–9.
2. Fridman G, Jost MM, Brooks AD, Fridman A, Gutsol A, Vasilets V, Friedman G. Floating electrode dielectric barrier discharge plasma in air promoting apoptotic behavior in melanoma skin cancer cell lines. Plasma Chem Plasma Process. 2007;27(2):163–76.
3. Service RF. Materials and biology. Nanotechnology takes aim at cancer. Science. 2005;310(5751):1132–4.
4. Rayavarapu RG, Petersen W, Ungureanu C, Post JN, van Leeuwen TG, Manohar S. Synthesis and bioconjugation of gold nanoparticles as potential molecular probes for light-based imaging techniques. Int J Biomed Imaging 2007;2007:29817.
5. Kim GC, Kim GJ, Park SR, Jeon SM, Seo HJ, Iza F, Lee JK. Air plasma coupled with antibody-conjugated nanoparticles: A new weapon against cancer. J Phys D. 2009;42(3):032005.
6. Daniels TR, Delgado T, Rodriguez JA, Helguera G, Penichet ML. The transferrin receptor part I: Biology and targeting with cytotoxic antibodies for the treatment of cancer. Clin Immunol. 2006;121(2):144–58.
7. Daniels TR, Delgado T, Helguera G, Penichet ML. The transferrin receptor part II: Targeted delivery of therapeutic agents into cancer cells. Clin Immunol. 2006;121(2):159–76.
8. Herbst RS. Review of epidermal growth factor receptor biology. Int J Radiat Oncol Biol Phys. 2004;59(2 suppl 1):S21–6.
9. Kim GJ, Kim W, Kim KT, Lee JK. DNA damage and mitochondria dysfunction in cell apoptosis induced by nonthermal air plasma. Appl Phys Lett. 2010;96:021502
10. Phillips DM. Determination of gas temperature from unresolved bands in the spectrum from a nitrogen discharge. J Phys D. 1976;9(3):507–21.
11. Ennis BW, Lippman ME, Dickson RB. The EGF receptor system as a target for antitumor therapy. Cancer Invest. 1991;9(5):553–62.
12. Herbst RS, Langer CJ. Epidermal growth factor receptors as a target for cancer treatment: the emerging role of IMC-C225 in the treatment of lung and head and neck cancers. Semin Oncol. 2002;(1 Suppl 4):27–36.
13. Kondapaka SB, Fridman R, Reddy KB. Epidermal growth factor and amphiregulin up-regulate matrix metalloproteinase-9 (MMP-9) in human breast cancer cells. Int J Cancer. 1997;70(6):722–6.